

## Binding Method for Detection of Muscarinic Acetylcholine Receptors in Receptor's Natural Environment

**Ikunobu Muramatsu, Hatsumi Yoshiki, Kiyonao Sada, Junsuke Uwada, Takanobu Taniguchi, Takayoshi Masuoka, and Matomo Nishio**

### Abstract

The pharmacological and biochemical properties of G protein-coupled receptors have been recently revealed to be more complex than originally supposed. Especially, in natural environment or in vivo, some receptors including muscarinic acetylcholine receptor (mAChR) are frequently modified by many factors, so that the receptors may exhibit multiple pharmacological profiles and biochemical functions, which are different from relatively constant and uniform properties originally reported in cell-free preparations and recombinant system. In order to detect the native properties of receptors occurring in tissues and cells without altering their natural environment and also to solve discrepancy between the functional affinity obtained by a bioassay approach and the binding affinity estimated from the conventional binding method with membrane preparations, the tissue segment binding method without homogenization has been recently developed as a new approach. In this chapter, the detailed protocol of tissue segment binding method and some unique properties of mAChRs observed in tissue segments are described.

**Key words** Radioligand binding, Tissue segments, Tissue homogenates, Muscarinic acetylcholine receptor (mAChR), Natural tissue environment, Affinity and density, Subcellular distribution

---

### 1 Introduction

The radioligand-binding method has been one of the most important techniques in studying the pharmacological characterization and biochemical identification of many types of receptors [1, 2]. This method was pioneered by Paton and Rang in 1965 [3], who incubated intact strips of intestinal smooth muscle with [<sup>3</sup>H]atropine, in order to study the ligand binding properties of mAChRs. However, the binding method was thereafter applied to homogenates or membrane fractions prepared from tissue, because receptor density is high in the membrane-rich preparations and any binding-interfering substances such as endogenous neurotransmitters could be removed in the fractionated preparations ([2], also see other chapters in this volume). Since the pharmacological

profiles of receptors obtained by the conventional membrane binding method are generally uniform among many tissues and relatively well consistent with those of recombinant receptors [2, 4], the conventional binding method with membrane preparations and the recombinant receptors have been widely employed for many purposes including the identification of receptors and the screening of drug candidates. However, there is emerging evidence that a receptor can show multiple pharmacological or biochemical properties under different conditions or states, in contrast to the uniform property supposed originally [5–10]. In particular, pharmacological specificity for some receptors may differ markedly between intact cells and cell-free preparations [11–13]. For example,  $M_3$ -mAChR subtype in rat cerebral cortex has relatively low affinity to  $M_3$ -selective antagonists (darifenacin and solifenacin) in the natural environment, while the antagonists can recognize the  $M_3$ -mAChRs with high affinity after homogenization [14]. Furthermore, there are often discrepancies in the native mAChRs between the functional affinities for antagonists obtained by a bioassay approach and the binding affinities estimated from the conventional membrane binding assay [15, 16]. Moreover,  $M_1$ -mAChR subtype has been recently demonstrated to exist and operate not only on the cell surface but also in intracellular sites in the central nervous system [17, 18]. The existence of functional intracellular mAChRs is inconsistent with a classical concept that mAChRs are representative cell-surface receptor. As tissue homogenization may cause disintegration of cell structure and/or dissociation with receptor and other membrane proteins and may result in significant changes of the pharmacological or biochemical properties, it seems very important to keep receptor's natural environment as possible. Recently, we have developed "intact tissue segment binding method" without homogenization [7, 19]. In this chapter, the detailed protocol of intact segment binding method and some unique profiles for native mAChRs are described.

---

## 2 Materials

### 2.1 Solution for Tissue Isolation

In order to maintain the native tissue environment, isotonic nutrient solutions have been used. We employ a modified Krebs–Henseleit solution that is commonly used in the functional bioassay. The composition is as follows: 121 mM NaCl, 5.9 mM KCl, 1.2 mM  $MgCl_2$ , 2.0 mM  $CaCl_2$ , 1.2 mM  $NaH_2PO_4$ , 25.5 mM  $NaHCO_3$ , and 11.5 mM glucose. The pH of the solution is maintained at 7.4 by gassing with 95 %  $O_2$  and 5 %  $CO_2$ . It is better to partially freeze the solution (0 °C) before tissue isolation in order to stop rapidly tissue/cell metabolism upon tissue isolation. Especially, brain must be placed in 0 °C solution immediately after isolation.

## 2.2 Incubation Buffer

The goal of using intact tissue in the tissue segment binding method is to keep the receptor environment closely as possible to that in tissues *in vivo*. Therefore, isotonic nutrient solutions are used during binding experiments. We use an incubation buffer (136 mM NaCl, 5.9 mM KCl, 1.2 mM MgCl<sub>2</sub>, 2.0 mM CaCl<sub>2</sub>, 1.2 mM NaH<sub>2</sub>PO<sub>4</sub>, 10.5 mM NaHCO<sub>3</sub>, and 11.5 mM glucose, pH 7.4 *in air*), whose composition is essentially the same as the modified Krebs–Henseleit solution described above. However, the incubation buffer cannot be aerated during the incubation period, in contrast to the case of a functional bioassay where the nutrient solution is bubbled with 95 % O<sub>2</sub> and 5 % CO<sub>2</sub>. Therefore, the NaHCO<sub>3</sub> concentration in the modified Krebs–Henseleit solution is reduced from 25.5 to 10.5 mM to adjust the pH to 7.4 under equilibration in room air, and the osmolality is compensated by adding NaCl. This bicarbonate buffer solution is sufficient to keep the pH constant under the incubation conditions at low temperature. Other isotonic solutions buffered with HEPES or Tris might be used instead of the bicarbonate buffer, but it should be tested before use whether the buffer composition affects the binding properties of the target receptors.

## 2.3 Radioligands

Two distinct radioligands have been used for the identification of mAChRs: 1-quinuclidinyl-[phenyl-4-<sup>3</sup>H]-benzilate ([<sup>3</sup>H]QNB) and 1-[N-methyl-<sup>3</sup>H]-scopolamine methyl chloride ([<sup>3</sup>H]NMS). [<sup>3</sup>H]QNB is hydrophobic and permeable through plasma membrane. Thus, as the proportion of nonspecific binding is significantly higher than that of hydrophilic [<sup>3</sup>H]NMS, [<sup>3</sup>H]NMS is useful to detect cell surface mAChRs. On the contrast, hydrophobic [<sup>3</sup>H]QNB can bind not only cell surface but also intracellular mAChRs [20–22]. In addition to radioligands, surface and intracellular mAChRs may be differently recognized by membrane-permeable atropine, or impermeable N-methylatropine or non-radioactive NMS, resulting in distinct proportions of nonspecific binding sites. Therefore, different combinations with radioligand and nonspecific ligand must be selected depending on research purposes (see Sect. 3) Radioligands and all tested drugs are diluted with incubation buffer before use. H<sub>2</sub>O must not be used for drug dilution. Glass tubes, but not plastic tubes, must be used for drug dilution and incubation (Fig. 1, step A), because *plastic tubes* may rapidly absorb radioligands and other tested drugs, resulting in a rapid reduction in their concentrations during dilution and incubation in contrast to glass tubes.

---

## 3 Methods

### 3.1 Preparation of Tissue Segments

The tissue segment binding method can be applied to all tissues isolated from animals including humans. Under a stereoscopic microscope and at 4 °C, surrounding unnecessary parts such as fat

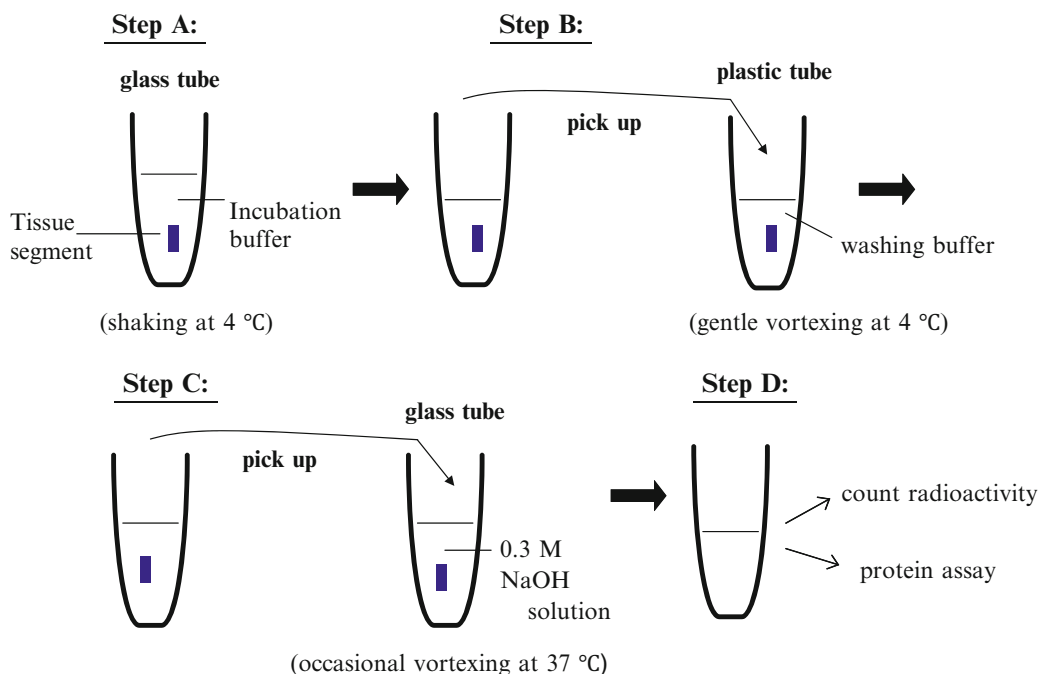


**Fig. 1** Experimental protocol for the tissue segment binding method. *Step A:* One tissue segment is incubated with [ $^3\text{H}$ ]NMS or [ $^3\text{H}$ ]QNB in the absence or presence of competitor in a glass tube at 4 °C. The incubation volume is generally 0.5 ml and the glass tube is shaken 110–120 times per min during incubation. Incubation periods (7–8 or 16 h) and combination of radioligand and competitor depend on the research purpose. *Step B:* Thereafter, the tissue segment is picked up by forceps, and then gently washed in a plastic tube containing a washing buffer at 4 °C for 40–60 s. *Step C:* The tissue segment is again picked up with another forceps, and then solubilized in 1 ml of 0.3 M NaOH solution at 37 °C for ~24 h. The test tube is strongly vortexed several times in order to facilitate the solubilization. *Step D:* After solubilization, the radioactivity and protein content are measured. In general, 500  $\mu\text{l}$  and 20–50  $\mu\text{l}$  of the solubilized solution are used for the measurements of radioactivity and protein content, respectively. *Thick horizontal arrows* between steps A and B, steps B and C, or steps C and D represent that the tubes described in both panels are the same, respectively

and connective tissues are removed. Muscle and mucosal layers can be separated in some tissues such as urinary bladder and stomach. Then the tissue is carefully cut into small pieces with ophthalmic fine scissors under a stereoscopic microscope. In order to allow diffusion of drug into tissue it is necessary to cut tissue in segments of small size. However, segments have to be big enough to keep receptor environment intact. Thus compromised size of sections has to be found. For example, the best size of rat cerebral cortex segments is approximately 1.5 mm in length, 1 mm in width, and 0.5 mm in thickness for the measurement of mAChRs. In rat detrusor and stomach muscles, the best size is 1  $\times$  1.5 mm although the thickness depends on the muscle layer.

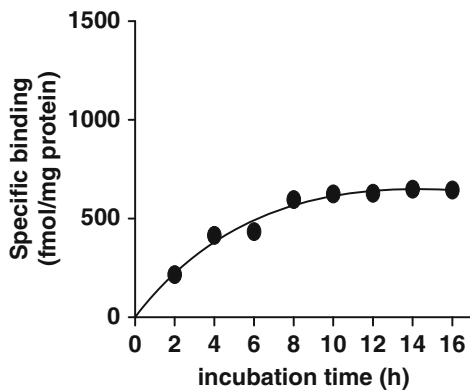
### 3.2 Incubation Volume and Temperature

As shown in Fig. 1, step A, one segment is incubated in one glass tube at 4 °C. The incubation volume is usually 0.5 or 1.0 ml, where a segment is incubated together with different concentrations of competitor and radioligand. In the tissues expressing receptor at high density, larger incubation volume (together with smaller size of tissue segments) is better to avoid a significant reduction of effective concentrations of radioligand and/or competitor added to the incubation solution during incubation. Incubation starts immediately after addition of radioligand. Incubation tubes are usually shaken 110–120 times per min. Some investigators consider 37 °C might be preferable, because this temperature is more physiological and because the resulting binding data might correspond better to the functional data measured at 37 °C. However, it must be noted that the intact tissue segments are incubated in an isotonic solution without bubbling air or oxygen. In order to rule out possible changes in natural states under anoxia at 37 °C, we have therefore used low temperature (generally 4 °C). Receptor trafficking seems to be neglected at this low temperature.

### 3.3 Incubation Time

In the conventional binding method with cell-free preparations, 2 h incubation is enough to reach equilibrium binding even at low temperature (4 °C). In contrast, binding process to intact tissue segments should be markedly influenced by tissue architecture and physicochemical properties of tested drugs. Figure 2 shows representative time course of specific binding of [<sup>3</sup>H]QNB in rat urinary bladder and cerebral cortex segments. At 1.5 nM of [<sup>3</sup>H]QNB, the binding to rat detrusor muscle is monophasic and reaches a plateau in incubation for approximately 8 h (Fig. 2a).

**a Urinary bladder**



**b Cerebral cortex**

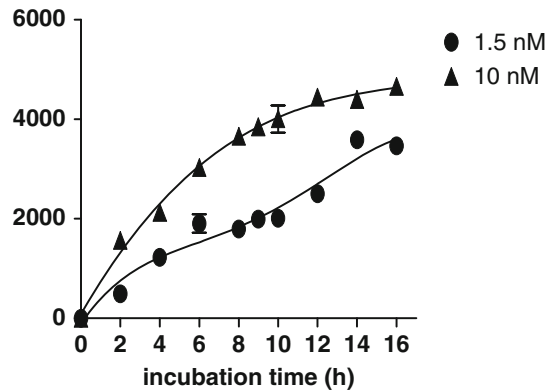


**Fig. 2** Time course of [<sup>3</sup>H]QNB binding to rat urinary bladder segments (**a**, detrusor muscle) and cerebral cortex (**b**) segments at 4 °C. [<sup>3</sup>H]QNB (1.5 nM in **a**, and 1.5 and 10 nM in **b**) was added at time 0 and then incubated for indicated periods. Specific binding was determined by subtraction of [<sup>3</sup>H]QNB binding in the presence of 1 μM atropine from total binding. Each point represents the mean of duplicate determinations and SEM in a representative experiment

However, the binding of 1.5 nM [ $^3\text{H}$ ]QNB to cerebral cortex is biphasic; the first plateau at approximately 8 h is followed by the second plateau at 16 h incubation (Fig. 2b). On the other hand, at a higher concentration (10 nM) of [ $^3\text{H}$ ]QNB, the binding increases monophasically in rat cerebral cortex segments (Fig. 2b). Recently, intracellular distribution of mAChRs in addition to cell surface has been demonstrated in rat, mouse and human brain and in neuroblastoma cells [17, 18], while mAChRs usually occur on the cell surface in the peripheral tissues such as urinary bladder when the receptors are not stimulated by agonists [21, 23–25]. Therefore, it is likely that monophasic binding of [ $^3\text{H}$ ]QNB at 10 nM reflects its faster penetration through plasma membrane and rapid association with mAChRs than those at low concentrations (1.5 nM) of [ $^3\text{H}$ ]QNB. Although different binding kinetics of QNB among mAChR subtypes cannot be also ruled out, the present and recent additional evidence suggests that the ability of hydrophobic [ $^3\text{H}$ ]QNB to bind to cell surface and intracellular mAChRs strongly depends on the plasma membrane permeability (physicochemical property) and concentrations of radioligand, and also on the incubation time. At present, we have used two different incubation periods (8 and 16 h) in [ $^3\text{H}$ ]QNB binding experiments in order to detect surface and total mAChRs. In this case, total number of mAChRs is estimated by subtracting non-specific binding defined with membrane-permeable atropine (1  $\mu\text{M}$ ) from total binding at 8 or 16 h incubation, while amount of surface mAChRs is calculated by subtracting the nonspecific binding defined with hydrophilic (membrane-impermeable) NMS (1  $\mu\text{M}$ ) at short incubation (8 h). Figure 3 shows the representative saturation curves for [ $^3\text{H}$ ]QNB binding to total and surface mAChRs in rat cerebral cortex segments, where similar total number of mAChRs can be estimated by atropine regardless of 8 or 16 h incubation (see more details in Sect. 4.2). Alternatively, surface mAChRs may be more specifically estimated from [ $^3\text{H}$ ]NMS binding to the segments, where nonspecific binding should be defined with the use of more hydrophilic N-methylatropine than atropine [21]. Combination of chemically same compounds (e.g., [ $^3\text{H}$ ]NMS vs. NMS) must be avoided in order to contaminate non-mAChR sites.

### 3.4 Washing

After incubation, each segment is carefully picked up by forceps from each incubation tube and quickly moved into a *plastic tube* containing ice-cold washing buffer (2 ml). Then, the plastic tubes are gently vortexed for 40–60 s (Fig. 1, step B). The washing buffer is the same as the incubation buffer used. Figure 4 shows the residual radioactivity remained in the tissue segments after washing for various times, where rat cerebral cortex segments were incubated with 2 nM [ $^3\text{H}$ ]NMS (a) or 2 and 10 nM [ $^3\text{H}$ ]QNB (b and c) in the absence or presence of 1  $\mu\text{M}$  atropine for 8 h beforehand. The residual radioactivity in the segments rapidly reduced after

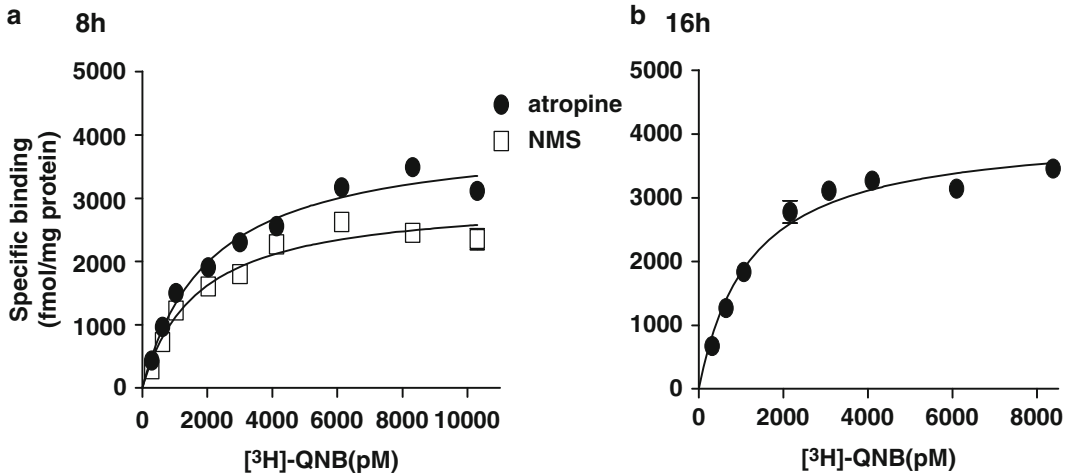


**Fig. 3** Representative saturation curves for [<sup>3</sup>H]QNB binding to intact segments of rat cerebral cortex. **(a)** The segments were incubated for 8 h and the specific binding (*circles* and *squares*) was determined by subtraction of [<sup>3</sup>H]QNB binding in the presence of 1 μM atropine or 1 μM NMS, respectively. **(b)** The segments were incubated for 16 h and specific binding (*circles*) was determined by subtraction of [<sup>3</sup>H]QNB binding in the presence of 1 μM atropine from total binding. Each point represents the mean of duplicate determinations and SEM in a representative experiment

washing and was maintained at relatively constant level during 15–120 s. It is interesting to note that tissue radioactivity before washing (at 0 s) is not so high as compared with the residual count after washing, suggesting that contamination of radioligand in extracellular/interstitial spaces is minor in the used segments. This conclusion is also supported by extremely low levels of nonspecific [<sup>3</sup>H]NMS binding in the segments incubated with atropine (Fig. 4a). In contrast, nonspecific binding of lipophilic [<sup>3</sup>H]QNB is higher in proportion than that of [<sup>3</sup>H]NMS, suggesting intracellular accumulation of [<sup>3</sup>H]QNB and its persistent retention during washing (Fig. 4b, c). After washing, the segment is picked up and moved into a *glass tube* for tissue solubilization (Fig. 1, step C). Different forceps must be used at steps B and C, in order to avoid possible contamination of radioligand. In the case of hard segments like muscle, the blotting on paper may be applied after picking up the segment.

### 3.5 Tissue Solubilization, and Measurement of Protein and Radioactivity

The washed segments are solubilized in 0.3 M NaOH solution (1 ml) to measure the bound radioactivity and the protein content (Fig. 1, steps C and D). Most of tissue segments are solubilized at 37 °C within 1 day. It must be noted that segment size varies among segments, that results in different protein concentrations between tubes. Therefore, protein content must be measured in every tube. In general, 10–50 μl of the solubilized tissue solution is used for protein assay and 500 μl for measurement of radioactivity of bound radioligand, respectively.

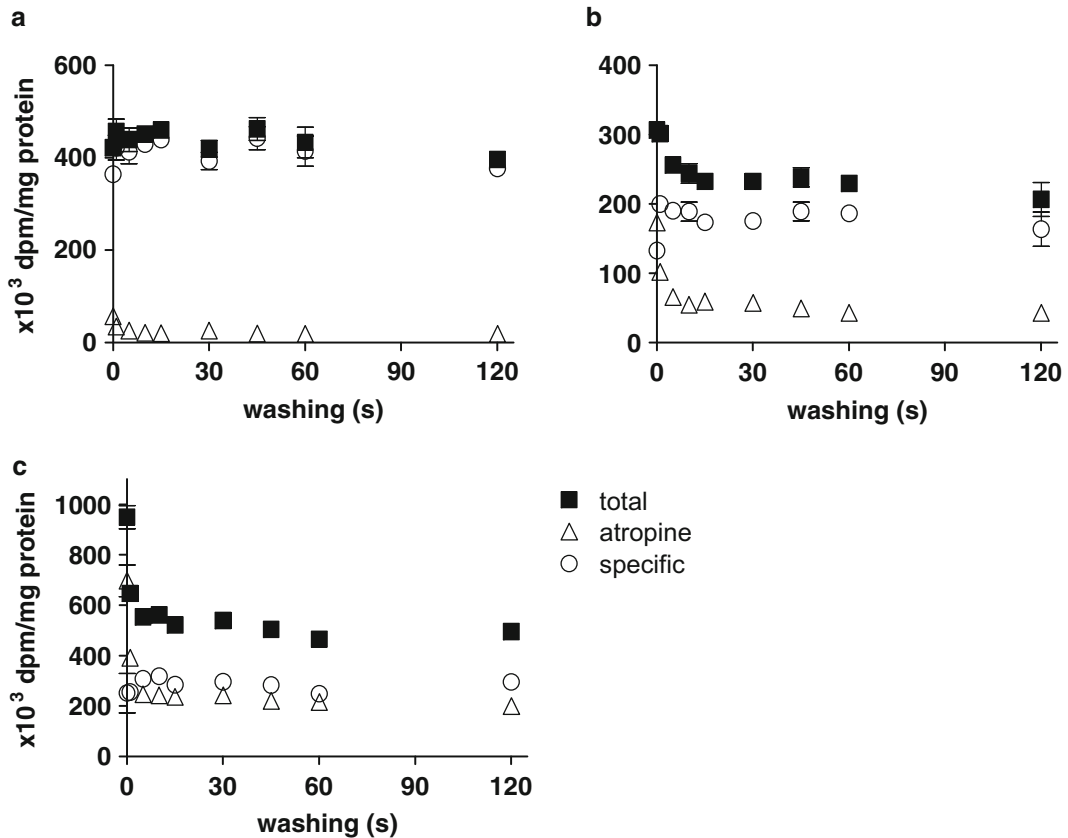


**Fig. 4** Residual radioactivity remained in the segments of rat cerebral cortex after washing. The segments were incubated with 2 nM [<sup>3</sup>H]NMS (**a**) or 2 and 10 nM [<sup>3</sup>H]QNB (**b** and **c**, respectively) for 8 h beforehand, and then picked up and washed for various times. In abscissa, time 0 means that the radioactivity of the segments was directly measured without washing. *Squares*: total radioactivity. *Circles*: specific radioactivity. *Triangles*: nonspecific radioactivity in atropine-treated segments. Each point represents the mean of duplicate determinations and SEM in a representative experiment

### 3.6 Data Analysis

Since each tissue segment varies in size, the solubilized tissue solution in each tube has different protein content. For normalization of the data, the radioactivity measured must be adjusted to the counts (dpm) bound per mg of protein. Then, binding data are analyzed using commercially available software (PRISM version 5.01; GraphPad Software, La Jolla, CA, USA) [7].

## 4 Notes

### 4.1 Binding Density and Affinity

The most important discrepancy between the tissue segment binding method and the conventional binding method using homogenates or microsomal fraction is a difference in binding density. Recent data of saturation binding experiments with [<sup>3</sup>H]NMS in



**Table 1**

**The dissociation constants ( $K_D$ ) and maximal binding capacities ( $B_{max}$ ) of [ $^3$ H]NMS in the intact segments and homogenates of various rat tissues**

| Tissue             | Segments   |                             | Homogenates  |                             |
|--------------------|------------|-----------------------------|--------------|-----------------------------|
|                    | $K_D$ (pM) | $B_{max}$ (fmol/mg protein) | $K_D$ (pM)   | $B_{max}$ (fmol/mg protein) |
| Cerebral cortex    | 1550       | 3000                        | 178<br>(134) | 2050<br>(1990)              |
| Striatum           | 2500       | 3700                        | 158          | 2800                        |
| Hippocampus        | 1800       | 2500                        | 197          | 1950                        |
| Cerebellum         | 350        | 280                         | 213          | 204                         |
| Submaxillary gland | 280        | 380                         | 185          | 153                         |
| Left ventricle     | 1050       | 420                         | 334<br>(163) | 86<br>(110)                 |
| Gastric muscle     | 970        | 1580                        | 245          | 550                         |
| Detrusor muscle    | 800        | 810                         | 212          | 226                         |

Saturation binding experiments were carried out at 4 °C. Incubation periods were 8 h in the segments and 2 h in the homogenates, respectively. Tissues were homogenized with the same buffer as the Krebs' incubation buffer used in the segment binding method, but cerebral cortex and left ventricle were also homogenized with Tris buffer (50 mM Tris, 2 mM EDTA, pH=7.4) and the data are shown in parentheses. Data represent mean value of 2–3 experiments

the segments and homogenates of various rat tissues are summarized in Table 1. Here, the tissues were homogenized either with the same Krebs' solution as the incubation buffer in the segment binding experiments or with sodium-free Tris-EDTA buffer in order to test the effects of distinct homogenizing buffers. When the binding capacities are compared using the same denominator (that is, per mg of total tissue protein in the segments and the homogenates), lower density of mAChRs can be estimated in the homogenates than in the segments, regardless of distinct homogenizing buffers. Similar differences in binding capacity have been reported in the mAChRs of other tissues (rat gastric mucosa [26]; human airways [27]; mouse epithelial cells [28]). Since the specific binding observed in segments is completely inhibited by not only lipophilic but also hydrophilic antagonists and agonists, higher density in the segments is not an overestimate due to nonspecific accumulation of radioligand into the tissue segments (see Sect. 3.4, Fig. 4). Rather, it is likely that the tissue segment binding method can avoid a yield loss of receptors which may be resulted from homogenization and/or membrane fractionation. This type of yield loss after homogenization has been reported in other receptors (nicotinic receptor [29];  $\alpha_1$ -adrenoceptor [19, 30–32];  $\beta$ -adrenoceptor [26, 33]). The improved yield of receptor in intact

segments is of particular value for dealing with limited amount of tissues and/or small animals. Recently, Ikeda et al. [27] have applied the segment binding method to human airway tissues in order to compare the distribution of mAChR and  $\beta$ -adrenoceptor subtypes between segmental and subsegmental bronchi (approximately 10 mm and 1–4 mm in outer diameter, respectively).

The second significant difference between both binding methods may be observed in binding affinities for radioligand or several drugs. Like [ $^3\text{H}$ ]QNB, [ $^3\text{H}$ ]NMS has been classically recognized as a non-selective but specific radioligand of mAChRs showing a relatively constant and high (subnanomolar) affinity in various tissues and recombinant receptors [4]; for example, 270 pM in rat cerebral cortex, 290 pM in rat hippocampus, 230 pM in rat corpus striatum, and 547 pM in rat gastric muscle [4, 14, 34, 35]. A similar high affinity (approximately 200 pM) for [ $^3\text{H}$ ]NMS was obtained in the present homogenate binding (Table 1). However, the dissociation constants for [ $^3\text{H}$ ]NMS estimated in the segments are relatively low and varied among the tested tissues (280–2500 pM). Besides these results, it has been reported that  $M_3$ -mAChRs in rat cerebral cortex cannot be identified as high affinity sites for  $M_3$  selective antagonists (darifenacin and solifenacin) under segmental conditions, while  $M_3$ -sites have been recognized as their high affinity sites in the homogenates or the membrane preparations [14]. Therefore, it is likely that tissue homogenization may cause a change in receptor profile in addition to yield loss, and it would in part explain well known discrepancy between functional bioassay and conventional binding assay. Although the mechanisms for yield loss and profile change after homogenization are not yet settled, it must be again emphasized that the segment-binding approach may shed light on distinct native phenotypes of cholinergic and probably other receptors observed in functional approach [7, 12, 13, 36].

#### **4.2 Identification of Surface and Intracellular mAChRs**

In contrast to peripheral tissues, the mAChRs in the cerebral cortex, striatum, and hippocampus exist not only on the cell membranes but also in the intracellular sites (mainly Golgi apparatus) [17]. The intracellular sites can be accessed by hydrophobic [ $^3\text{H}$ ]QNB but not by hydrophilic [ $^3\text{H}$ ]NMS [20–22]. Figure 3a shows representative saturation curves for [ $^3\text{H}$ ]QNB binding in rat cerebral cortex segments under 8 h incubation, where two distinct binding capacities are estimated using hydrophilic (membrane-impermeable) unlabeled NMS and membrane-permeable atropine, respectively. The density estimated with hydrophilic NMS is significantly lower than that estimated with atropine. Such a high density of mAChRs is also obtained under long incubation (16 h) in the absence or presence of atropine (Fig. 3b). These differences in binding capacities are also observed in striatum and hippocampus of rats and mice, but not in the cerebellum and peripheral tissues.

These results suggest that mAChRs are localized not only on the cell surface but also at intracellular sites in some brain areas, and that such distinct subcellular distribution of mAChRs can be identified by different combinations of [<sup>3</sup>H]QNB with hydrophobic and/or hydrophilic ligands in the segments. In reference to this point, it is important to emphasize repeatedly that cell surface and intracellular receptors cannot be discriminated after homogenization. Detection of distinct subcellular distribution of receptors would be influenced by physicochemical property and concentrations of ligands, and incubation times.

### 4.3 Summary and Perspective

Under natural/physiological environment, mAChRs and probably other receptors may exist and function as pharmacologically distinct phenotypes which are different from relatively constant and uniform profile observed in homogenized tissues or recombinant system. The tissue segment binding method is a powerful tool for detecting the native properties of receptors occurring in tissues and cells without altering their environment, and would provide important information of pharmacokinetic analysis, positron emission tomography (PET) analysis and in drug development. Recently, it has been suggested that *in vivo* distribution of receptor ligands may be related to the distinct binding affinities estimated in the segments of various tissues but not to a uniform affinity estimated in the homogenates [13].

---

## Acknowledgments

This work was supported in part by a Grant-in-Aid for Scientific Research from Japan Society of the Promotion of Science (JSPS), a grant from the Smoking Research Foundation of Japan, and Organization for Life Science Advancement Programs, University of Fukui.

## References

1. Yamamura HI, Enna SJ, Kuhar MJ (eds) (1985) Neurotransmitter receptor binding, 2nd edn. Raven Press, New York
2. Bylund DB, Deupree JD, Toews ML (2004) Radioligand-binding methods for membrane preparations and intact cells. *Methods Mol Biol* 259:1–28
3. Paton WDM, Rang HP (1965) The uptake of atropine and related drugs by intestinal smooth muscle of the guinea-pig in relation to acetylcholine receptors. *Proc R Soc Lond B Biol Sci* 163:1–44
4. Alexander SPH, Mathie A, Peters JA (2009) Guide to Receptors and Channels (GRAC), 4th edition. *Br J Pharmacol* 158(suppl):S1–S254
5. Kenakin T (1995) On the importance of the “antagonist assumption” to how receptors express themselves. *Biochem Pharmacol* 55:17–26
6. Kenakin T, Miller LJ (2010) Seven transmembrane receptors as shape shifting proteins: the impact of allosteric modulation and functional selectivity on new drug discovery. *Pharmacol Rev* 62:265–304

7. Muramatsu I, Tanaka T, Suzuki F, Li Z, Hiraizumi-Hiraoka Y, Anisuzzaman ASM, Yamamoto H, Horinouchi T, Morishima S (2005) Quantifying receptor properties: the tissue segment binding method—a powerful tool for the pharmacome analysis of native receptors. *J Pharmacol Sci* 98:331–339
8. Baker JG, Hill SJ (2007) Multiple GPCR conformations and signaling pathways: implications for antagonist affinity estimates. *Trends Pharmacol Sci* 28:374–381
9. Nelson CP, Challiss RAJ (2007) “Phenotypic” pharmacology: the influence of cellular environment on G protein-coupled receptor antagonist and inverse agonist pharmacology. *Biochem Pharmacol* 73:737–751
10. Lane JR, Sexton PM, Christopoulos A (2013) Bridging the gap: bitopic ligands of G-protein-coupled receptors. *Trends Pharmacol Sci* 34:59–66
11. Toung MDT, Garbarg M, Schwartz JC (1980) Pharmacological specificity of brain histamine H<sub>2</sub>-receptors differs in intact cells and cell-free preparations. *Nature* 287:548–551
12. Nishimune A, Yoshiki H, Uwada J, Anisuzzaman AS, Umada H, Muramatsu I (2012) Phenotype Pharmacology of lower urinary tract  $\alpha_1$ -adrenoceptors. *Br J Pharmacol* 165:1226–1234
13. Yoshiki H, Uwada J, Anisuzzaman ASM, Umada H, Hayashi R, Kainoh M, Masuoka T, Nishio M, Muramatsu I (2014) Pharmacologically distinct phenotypes of  $\alpha_{1B}$ -adrenoceptors: variation in binding and functional affinities for antagonists. *Br J Pharmacol* 171:4890–4901
14. Anisuzzaman ASM, Nishimune A, Yoshiki H, Uwada J, Muramatsu I (2011) Influence of tissue integrity of pharmacological phenotypes of muscarinic acetylcholine receptors in the rat cerebral cortex. *J Pharmacol Exp Ther* 339:186–193
15. Boxall DK, Ford AP, Choppin A, Nahorski SR, Challis RA, Eglen RM (1998) Characterization of an atypical muscarinic cholinergic receptor mediating contraction of the guinea-pig isolated uterus. *Br J Pharmacol* 124:1615–1622
16. Munns M, Pennefather JN (1998) Pharmacological characterization of muscarinic receptors in the uterus of oestrogen-primed and pregnant rats. *Br J Pharmacol* 123:1639–1644
17. Uwada J, Anisuzzaman AMS, Yoshiki H, Nishimune A, Muramatsu I (2011) Intracellular distribution of functional M1-muscarinic acetylcholine receptors in N1E-115 neuroblastoma cells. *J Neurochem* 118:958–967
18. Anisuzzaman AMS, Uwada J, Masuoka T, Yoshiki H, Nishio M, Ikegaya Y, Takahashi N, Matsuki N, Fujibayashi Y, Yonekura Y, Momiyama T, Muramatsu I (2013) Novel contribution of cell surface and intracellular M1-muscarinic acetylcholine receptors to synaptic plasticity in hippocampus. *J Neurochem* 126:360–371
19. Tanaka T, Zhang L, Suzuki F, Muramatsu I (2004) Alpha-1 adrenoceptors: evaluation of receptor subtype-binding kinetics in intact arterial tissues and comparison with membrane binding. *Br J Pharmacol* 141:468–476
20. Galper JB, Dziekan LC, O’Hara DS, Smith TW (1982) The biphasic response of muscarinic receptors in cultured heart cells to agonists. Effects on receptor number and affinity in intact cells and homogenates. *J Biol Chem* 257:10344–10356
21. Koenig JA, Edwardson JM (1996) Intracellular trafficking of the muscarinic acetylcholine receptor: importance of subtype and cell type. *Mol Pharmacol* 49:351–359
22. Dessy C, Kelly RA, Balligand JL, Feron O (2000) Dynamic mediates caveolar sequestration of muscarinic cholinergic receptors and alteration in NO signaling. *EMBO J* 19:4272–4280
23. Anisuzzaman ASM, Morishima S, Suzuki F, Tanaka T, Yoshiki H, Sathi ZS, Akino H, Yokoyama O, Muramatsu I (2008) Assessment of muscarinic receptor subtypes in human and rat lower urinary tract by tissue segment binding assay. *J Pharmacol Sci* 106:271–279
24. Uwada J, Yoshiki H, Masuoka T, Nishio M, Muramatsu I (2014) Intracellular localization of M1 muscarinic acetylcholine receptor through clathrin-dependent constitutive internalization via a C-terminal tryptophan-based motif. *J Cell Sci* 127:3131–3140
25. Van Koppen CJ, Kaiser B (2003) Regulation of muscarinic acetylcholine receptor signaling. *Pharmacol Ther* 98:197–220
26. Anisuzzaman ASM, Morishima S, Suzuki F, Tanaka T, Muramatsu I (2008) Identification of M1 muscarinic receptor subtype in rat stomach using a tissue segment binding method, and the effects of immobilization stress on the muscarinic receptors. *Eur J Pharmacol* 599:146–151
27. Ikeda T, Anisuzzaman AMS, Yoshiki H, Sasaki M, Koshiji T, Nishimune A, Muramatsu I (2012) Regional quantification of muscarinic acetylcholine receptors and  $\beta$ -adrenoceptors in human airway. *Br J Pharmacol* 166:1804–1814
28. Khan RIM, Anisuzzaman AMS, Semba S, Ma Y, Uwada J et al (2013) M1 is a major subtype of muscarinic acetylcholine receptors on mouse epithelial cells. *J Gastroenterol* 48:885–896
29. Wang MH, Yoshiki H, Anisuzzaman ASM, Uwada J, Nishimune A, Lee KS, Taniguchi T, Muramatsu I (2011) Re-evaluation of nicotinic

- acetylcholine receptors in rat brain by a tissue-segment binding assay. *Front Pharmacol* 2:65. doi:[10.3389/fphar.2011.00065](https://doi.org/10.3389/fphar.2011.00065)
30. Colucci WS, Gimbrone JRMA, Alexander RW (1981) Regulation of the postsynaptic alpha-adrenergic receptor in rat mesenteric artery. Effects of chemical sympathectomy and epinephrine treatment. *Circ Res* 48:104–111
  31. Faber JE, Yang N, Xin XH (2001) Expression of  $\alpha$ -adrenoceptor subtypes by smooth muscle cell and adventitial fibroblast in rat aorta and in cell culture. *J Pharmacol Exp Ther* 298:441–452
  32. Hiraizumi-Hiraoka Y, Tanaka T, Yamamoto H, Suzuki F, Muramatsu I (2004) Identification of  $\alpha$ -1L adrenoceptor in rabbit ear artery. *J Pharmacol Exp Ther* 310:995–1002
  33. Horinouchi T, Morishima S, Tanaka T, Suzuki F, Tanaka Y, Kioko K, Muramatsu I (2006) Pharmacological evaluation of plasma membrane  $\beta$ -adrenoceptors in rat hearts using the tissue segment binding method. *Life Sci* 79: 941–948
  34. Delmendo RE, Michel AD, Whiting RL (1989) Affinity of muscarinic receptor antagonists for three putative muscarinic receptor binding sites. *Br J Pharmacol* 96:457–464
  35. Ehlert FJ, Tran LP (1990) Regional distribution of M1, M2 and non-M1, non-M2 subtypes of muscarinic binding sites in rat brain. *J Pharmacol Exp Ther* 255:1148–1157
  36. Sathi ZS, Anisuzzaman ASM, Morishima S, Suzuki F, Tanaka T, Yoshiki H, Muramatsu I (2008) Different affinities of native  $\alpha$ 1B-adrenoceptors for ketanserin between intact tissue segments and membrane preparation. *Eur J Pharmacol* 584:22–228